QIRT 2018
10.21611/qirt.2018.006
14th Quantitative InfraRed Thermography Conference

Active thermography for quality assurance of 3D-printed polymer structures

by C. Metz*, P. Franz*, C. Fischer**, V. Wachtendorf*, C. Maierhofer*

* Bundesanstalt für Materialforschung und -prüfung (BAM), Unter den Eichen 87, 12205 Berlin, Germany, *christian.metz@bam.de*
**SKZ - Das Kunststoffzentrum, Friedrich-Bergius-Ring 22, 97076 Würzburg, Germany, *c.fischer@skz.de*

Abstract

Additively manufactured test specimens made of polyamide 12 (PA 12) by Laser Sintering (LS) as well as of acrylnitril-butadien-styrol (ABS) by Fused Layer Modeling (FLM), were tested with active thermography. For this, two different excitation methods (flash and impulse excitation) were used and compared, regarding the suitability for the detection of constructed and imprinted defects. To increase the quality of the thermograms, data processing methods like thermal signal reconstruction (TSR) and Fourier-Transformation were applied. Furthermore, the long-term stability of the probes towards environmental stress, like UV-radiation, heat, water contact and frost is being investigated in the presented project with artificial weathering tests.

1. Introduction

Additive manufacturing (AM) is an uprising technique, which is developing very fast [1,2]. Due to the advanced state of the technical development, the speeding up of computational efficiency and the expiring of patents, the availability of AM has reached small and medium-sized enterprises and even private persons. Besides the usage of new materials and new methods, the application also shifts from prototyping to the production of individual and even serial parts. However, small-batch production (starting at quantities of 1 piece) of technical parts, that have to face e. g. mechanical and environmental stress, demands a much higher accuracy and long-term stability than the production of prototypes. In AM, the layer-by-layer production causes differences in the resulting material properties compared to parts made by conventional production methods. In particular physical properties (porosity, density, strength, thermal conductivity, specific heat capacity, electrical conductivity etc.), surface properties (roughness, shape of edges, surface chemistry, etc.), the anisotropy of the chemical composition especially the horizontal and vertical distribution of thermo-oxidized species, the anisotropy of the molecular orientation (horizontal and vertical), as well as chemical resistance towards environmental stress (aging processes) may be affected. Therefore, a reliable and non-destructive quality assurance is needed, to guarantee for the demanded properties of the additively manufactured parts. Only faultless, secure and reliable manufactured parts can prevail in economy [3].

This joint AiF-IGF project presented here focusses on the properties of additively manufactured plastic parts, and how these properties change under varying conditions of the manufacturing process as well as during the aging process after manufacturing. Test specimens made of PA 12 produced by LS and test specimens made of ABS produced by FLM were manufactured at SKZ (-Das Kunststoffzentrum) and examined at BAM (Bundesanstalt für Materialforschung und -prüfung). Currently, LS and FLM are the two most important additive manufacturing techniques for polymeric materials in industry, especially for small and medium sized enterprises [4,5]. The main objective of the project is the development of strategies for quality assurance based on non-destructive characterization of the material properties depending on the process parameters and on long term ageing. This needs knowledge about the change in properties that go together with the variation of production parameters like the composition of the raw materials or the printing speed. To assure the durability of additively manufactured plastic parts, the change of the properties during the exposure to environmental stress is investigated.

To account for this, artificial weathering of the test specimens is done under defined criteria, while monitoring their property changes in reference to their respective unexposed state. The test specimens were therefore fully characterized with non-destructive testing (NDT) methods like active thermography (thermal testing, TT) and imaging ultrasound (ultrasonic testing, UT) as well as spectroscopic methods like ATR-IR-spectroscopy, UV/VIS-spectroscopy, and spectral reflection. To find strategies for a quality assurance, TT will be used for the detection of defects and the capabilities, conditions and technical limits of this method will be explored. Additionally, the mechanical properties will be tested, which is only possible with destructive testing.

2. Additive manufacturing of test specimens

In AM, a 3D part is generated through an iterative layer-by-layer production. Therefore, the virtual structure of the part gets sliced into layers by a software. These layers are all horizontal and parallel, so that the printer-head or the laser only has to move in the 2-dimensional x-y-plane, to create one single layer. In this way it is often possible to save raw material and to realize geometries of parts, that were impossible to generate with conventional manufacturing methods like plastic injection moulding or others. The two already mentioned additive manufacturing techniques LS and FLM, which were used in this project, will now be described shortly.

2.1. Laser-Sintering (LS)

In the LS-method a thermoplastic polymer powder is evenly distributed with a squeegee in a production chamber, filled with inert gas, to create a horizontal powder layer (powder bed) [4]. This layer is always heated up to a temperature shortly below the melting point of the plastic and typically has a thickness between 60 µm and 200 µm. In the next step, an infrared laser (wavelength 10.6 µm) draws one layer of the previous sliced part structure into the powder bed and so locally converts the plastic from a solid and partly crystalline phase into an amorphous, liquid phase. Once the laser has scanned the complete structure layer, the powder bed is lowered in z-direction by the amount of the next layer thickness. The squeegee then establishes a new horizontal powder layer and the iterative process starts again. As the structure gets drawn into an evenly distributed powder layer, the powder serves as a mechanical support for the unfinished part under construction and cavities in the final manufactured part will be filled with unmolten powder. After the printing process and a cooling phase, the residual powder around the printed part has to be removed and can be partially reused in the next printing job, after thoroughly mixing with a certain amount of freshly produced powder. As the plastic powder is quite expensive, the amount of recyclable material severely affects the overall cost of the printing job.

Compared with FLM, it is possible to print very delicate and thin structures with LS, provided that the laser is focussed well and the powder layers are thin. Due to the complexity of the production processes, however, the number of suitable plastics is limited and the machines are comparably big and expensive. An unpigmented PA 12 blend, that was optimised for the AM process therefore can be seen as a standard for LS at the moment and was also used to generate the test specimens in the project.

2.2. Fused Layer Modeling (FLM)

The polymer to be printed in the FLM method has the form of a long filament wire, which is wound up on a spool [6]. It typically has a diameter of 1.75 mm or 2.85 mm and is guided through the printer head into an extruder with a heated nozzle. As a short region before the nozzle is already hot enough to melt the plastic, the unmolten filament itself serves as a piston to press the molten plastic through the nozzle. Therefore, the speed with which the filament is drawn into the printer head, directly affects the amount of extruded plastic per time, although the extruder is able to pause the flow by a sudden retraction of the unmolten filament. In this way, the molten plastic strand gets deposited on the printer bed, which is a heated, plain surface (typically aluminium or glass laminated with adhesive tape or other coatings) to form one horizontal x-y-layer. Once a line-by-line drawn layer of the part is finished, the printer head is altered (or the printing bed is lowered) in z-direction by the amount of the thickness of one layer. As there is no surrounding polymer powder like in LS, a supporting structure has to be printed at regions, where the overhang of the shape of the part exceeds a certain angle. This supporting structure has to be removed after the printing job is finished. Also, there is no inert gas and often not even a closed printing chamber. Cavities in the finished part are therefore filled with air.

Besides the AM of parts and prototypes in the industry, FLM printers are also used in the private sector, where it is colloquially often referred to as 3D-printing. The resolution of the FLM-printed parts is lower, compared with LS, which is primarily due to the diameter of the nozzle, whereas the variety of suitable polymers is higher. For this project, ABS was chosen.

2.3. Test Specimens

The test specimens were printed as step wedges (60 x 160 mm) with four steps (step heights of 1, 2, 4 and 8 mm), see figure 1. In every step, six artificial cylindric defects with different diameters were included. The defect height was 0.6 mm over the whole specimen. Another set of specimens was realized with the same defect positions and diameters, but a defect height of 0.2 mm. In figure 1 (*left*), a sketch (stretched in z-direction for better display) of the step wedges can be seen, which were printed in unpigmented PA 12 (LS) and red colored ABS (FLM). Additionally, a set of step wedges were printed without any defects for comparison.

The weathering exposure, however, were done on step wedges with different geometry (pictures not shown) and made of unpigmented PA 12 (LS) and unpigmented ABS (FLM), respectively. Two sets of specimens (step wedges) were additively manufactured, one set with three steps (step heights of 2, 4 and 8 mm) and six artificial cylindric defects on every step and another set without any artificial defects (step heights of 1, 2 and 4 mm). The cylindrical defects were placed centric in z-direction, equally to the step wedges with four steps. Three of them, however, were 0.6 mm in height (diameters: 2, 4 and 6 mm) and three of them were 0.2 mm in height (diameters: 2, 4 and 6 mm) on every step.

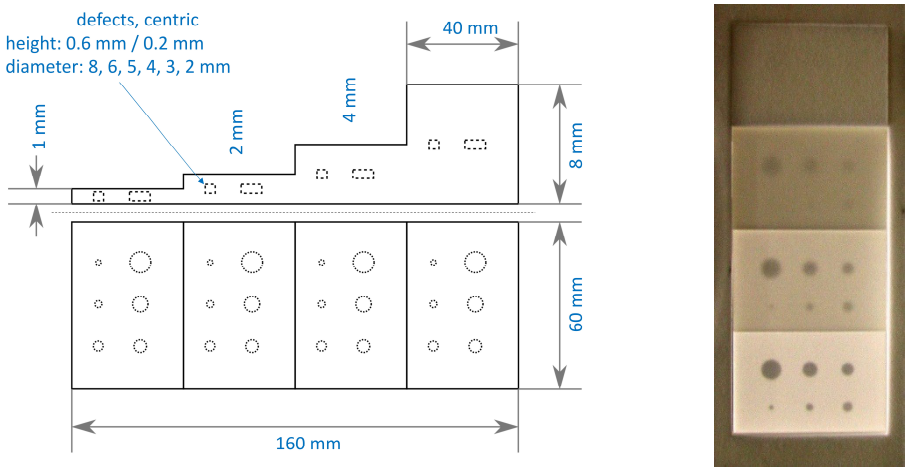

Fig. 1. *Left: Sketch of a test specimen, side view (stretched in z-direction) and top view. There are cylindric defects included, centric z-direction in every step but with varying diameters (8, 6, 5, 4, 3, 2 mm). The defect height (0.6 mm) is the same for all defects. A second defect height (0.2 mm) was realized in a second set of specimens. The specimens were made of unpigmented PA 12 (LS-method) and of red colored ABS (FLM-method). Right: Photo of a PA 12 step wedge specimen with artificial defects (height 0.6 mm), top view. Some defects are recognizable in transmitted light.*

As the two AM methods, LS and FLM, have process-specific differences, the imprinted artificial defects in the step wedges also differ regarding their content. The step wedges made of PA 12 with LS had defects, which were filled with unmolten plastic powder, because the powder is distributed equally in every layer during the printing process. The defects are therefore cavities inside the part, from which the powder cannot be removed. The defects in the step wedges made of ABS (FLM) however, were only filled with air. The extruder in the FLM-printer head is able to retract the plastic filament and, in this way, to stop the plastic flow temporarily.

For comparison, reference step wedges without any defects made of PA 12 and ABS were also produced with plastic injection moulding, a conventional production method.

As the mechanical properties can only be determined by a destructive tensile testing, tension rods were also produced in the project with LS, FLM and injection moulding. All specimens were manufactured at SKZ – Das Kunststoffzentrum in Würzburg, Germany.

2.4. Artificial weathering

To test the durability of the AM plastic parts, the specimens were exposed to an artificial aging procedure. They were placed in a fluorescent UV lamp device of the type Global UV Test 200 (Weiss Umwelttechnik GmbH, Reiskirchen, Germany), based on ISO 4892-3 [7], with UV-A fluorescent lamps (340 nm) for 2000 hours (~3 months). This artificial exposure is equivalent in terms of UV radiant exposure to a natural weathering of a couple of years. With this device it is possible to control the temperature, the humidity as well as rain phases, and the UV-radiation intensity. The short-wave edge of the spectrum of the UV-lamps corresponds to the spectral distribution of the global radiation. A repeating 24-h-cycle was carried out, in which a rain phase at 25 °C temperature was followed by a dry phase at 50 °C for two times and after that, the temperature was lowered to -10°C to introduce mechanical stress into the specimens. Meanwhile, the UV-irradiation was kept constant during the whole cycle.

During the artificial aging process, all parameters (temperature, humidity, wavelength and radiation intensity) were kept in the ranges to be found in the normal outside environment. The speeding up of the artificial aging was reached only by the time-compression of the most stressing phases and the constant UV-irradiation, which would not be possible in an outdoor weathering experiment. Another advantage is that all conditions during an artificial weathering experiment can be controlled and are therefore repeatable and reproducible.

While UV-irradiation has the highest potential among the exposure parameters and can cause the cleavage of chemical bonds and induce oxidation reactions with the surrounding air, it is expected that the enduring contact with water and humidity might wash out additives from the specimens on the one hand and favour the water ingress and therefore hydrolysis reactions on the other hand. All specimens were examined before the start of the weathering experiment with the mentioned analytical methods. To monitor the progress of the changes of the material properties, all specimens are examined and tested after the first third (667 h or ~ 1 month) and after the second third (1333 h or ~ 2 months) of the whole weathering time and again after the experiment is finished.

3. Experimental

3.1. Thermal testing, TT

TT measurements were made in both experimental setups, reflection and transmission configuration, in each case with flash excitation as well was with impulse excitation using halogen lamps. For this, an Infratec ImageIR 8800 Infrared(IR)-camera system with a cooled Mercury-Cadmium-Telluride (MCT) focal plane array detector with a sensitive spectral range from 8 µm to 9.4 µm (long-wavelength infrared, LWIR) was used. The excitation sources were provided with infrared filters made of PMMA to avoid disturbing thermal radiation.

For flash excitation, four Hensel EH Pro 6000 flash lamps were placed in 40 cm distance to the specimens. The pulse length of the flash was in the range of 3 ms and the energy supply for one flash lamp was 6 kJ. The impulse excitation was done with two Hedler H25s halogen lamps with a power of 2 kW each, placed in 50 cm distance to the test specimens. For the excitation time, 15 s and 30 s were chosen and the pulse shape was recorded with a silicon photo diode. The IR camera recording always started before the beginning of the excitation. The whole recording conditions are shown in Table 1.

Table 1. Recording conditions for thermal testing.

Excitation	Pulse length	Distance excitation source to specimen	Distance specimen to IR camera	Recording time	Frame rate
Flash	~ 3 ms	40 cm	50 cm	240 s	25 Hz
Impulse (halogen)	15 s and 30 s	50 cm	55 cm	160 s	25 Hz

3.2. Spectral reflection

Reflection spectra between 360 nm and 740 nm were recorded with a Minolta CM-2600 d spectrophotometer (KONICA MINOLTA SENSING, INC), wavelength pitch: 10 nm, measurement time 1.5 s. This device works with three pulsed xenon flash lamps and allows for the precise and reproducible determination of the reflection spectrum of the specimen surface. As both plastics, PA 12 and ABS, are partially transparent at least in the visible light spectrum, all specimens were measured lying on a black surface.

3.3. UV/VIS spectroscopy

UV/VIS transmission spectra between 220 nm and 700 nm were recorded with a Varian UV-VIS spectrometer Cary 300 with a spectral resolution of 0.2 nm, a wavelength accuracy of 0.02 to 0.04 nm, UV-Vis Data interval of 1.0 nm, and a S/N time out of 10 seconds. Only the 1 mm thick steps of each specimen could be measured, because the extinction in thicker probe parts was too high. In the experimental setup, an integrating sphere was used to collect straylight and refracted light after its transition through the sample.

4. Results

4.1. Partial transparency and aging effects

The aging of plastics is a very complex process and its course depends on many parameters, like the chemical stability, the meso- and microstructure of the surface, the duration of exposure to environmental stress like UV-radiation (intensity and wavelength) or water contact, just to mention a few. Moreover, plastics are a complex mixture of polymers, additives, fillers and other substances, so that the way of production and additionally the way of processing of plastics may also influence the resulting part. Also, as far as the exposure a strong synergism in its effects means that the various exposure parameters have to act simultaneously and in parallel. While the underlying molecular changes are the same, the expression of weathering effects is different for different properties. Therefore, it is necessary to look at the change of every single property individually during the aging process, as far as this is possible. As spectroscopic methods are sensitive to chemical alterations, spectral reflection, UV/VIS- and ATR-IR-spectroscopy have been applied.

In figure 2, three exemplary UV/VIS spectra of 1 mm thick unpigmented PA 12 (for LS), of red colored ABS and of unpigmented ABS (for FLM) are shown shortly after they were additively manufactured. Both polymers have an absorption edge in the visible spectral range, at 400 nm for unpigmented PA 12, at 620 nm for red colored ABS and between 330 nm and 290 nm for unpigmented ABS. At higher wavelengths, the absorbance goes below 1, which means that, depending on refraction and reflection, a significant amount of radiation passes through the material without interaction. This means that both materials, PA 12 and ABS are partially transparent in these spectral regions.

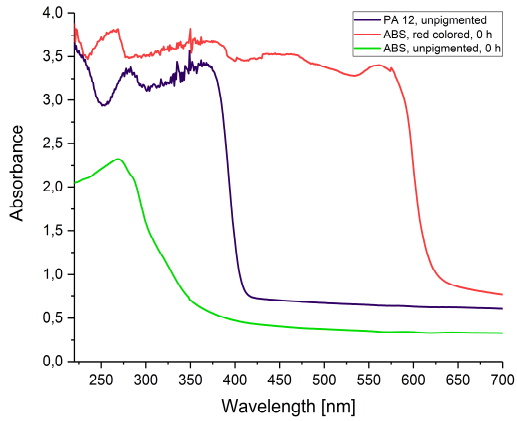

Fig. 2. *UV/VIS spectra of 1 mm thick unpigmented PA 12 (purple), red colored ABS (red) and unpigmented ABS (light green). Both materials are partially transparent.*

In figure 3 (left), UV/VIS spectra of unpigmented ABS, shortly after additive manufacturing of the specimen (light green) is compared with the same probe after 667 hours of weathering under the procedure and conditions described above (dark green). The difference spectrum is shown in red. As the material was exposed to the weathering process, the absorption edge shifted to longer wavelengths. The opaque region broadened and its absorbance increased.

On the right side in figure 3, the corresponding spectral reflection spectra of undamaged and aged ABS (unpigmented), as well as the difference spectrum, are shown. The unit “SCI” in the diagram stands for “specular component included”, which indicates both, the *diffuse* reflection as well as the *specular* reflection of light by a surface.

After the weathering experiment, the reflection in the shorter wavelengths region (roughly 450 nm and shorter) decreased. This means, that in this spectral region less radiation was reflected from the surface of the specimen, because absorption in the blue occurred during the aging process leading to a yellow discoloration.

The combination of the UV/VIS-spectra and spectral reflection information show that more radiation energy was absorbed by unpigmented damaged ABS, compared to unpigmented undamaged ABS. However, there was still a high partial transparency left, even after 667 hours of intensive artificial weathering.

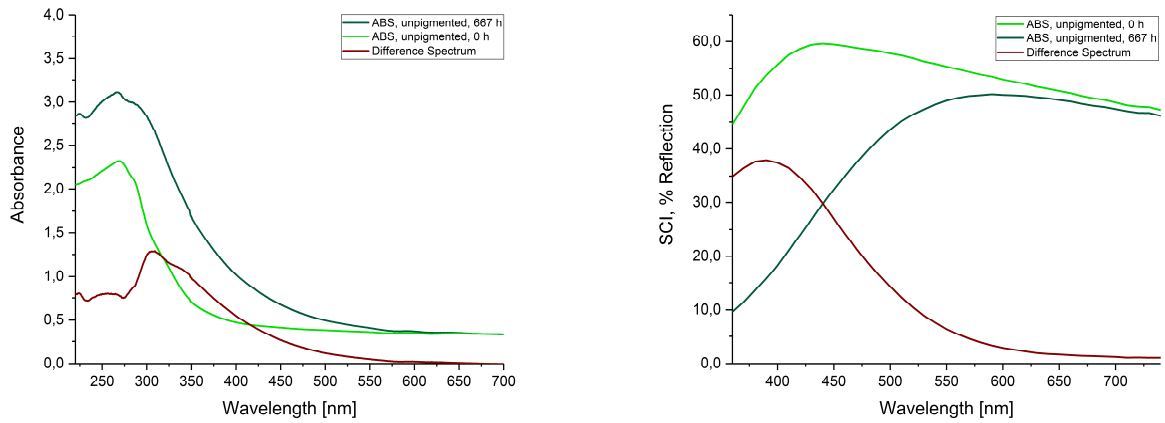

Fig. 3. *UV/VIS spectra (left) and spectral reflection data (right) for a 1 mm thick step of unpigmented ABS after production with AM (light green), after 667 hours of artificial weathering (dark green) and the difference spectrum (red). The partial transparency decreased, when ABS was damaged during artificial weathering.*

4.2. Thermal testing: detection of defects

The above mentioned partial transparency also occurred at higher wavelengths (not shown) but was lower in the LWIR (here: 8 µm to 9 µm) than in the MWIR (from 3 µm to 5 µm) [8, 9]. It is a major problem to TT using optical excitation with flash and halogen lamps, because the energy from the excitation source is not transformed into heat on the surface completely, as it would be in the ideal case. Additionally, radiation can be transformed into heat in the inside of the material, what makes calculations more complex and has to be considered in theory and data reconstruction [10].

In the following, only results from TT reflection measurements obtained with flash and halogen impulse excitation on two step wedges of unpigmented PA 12 and red colored ABS, both undamaged, shortly after additive manufacturing and before the weathering experiment, are shown (figures 4 to 7). The plain side of the step wedges were oriented towards the IR camera and the cylindrical defects inside the specimens were 0.6 mm in height at both specimens. For data analysis, first a thermogram recorded b efore optical heating was subtracted from the whole thermogram sequence. Thus, only temperature increases due to heating are shown in the following thermograms. For each step wedge, those thermograms were selected and displayed showing the deepest defects with maximum contrast. Further data processing steps with the aim of improving the signal-to-noise ratio of the defects were performed as described for each figure in more detail in the following.

Zero image correction, hybrid-median-filter

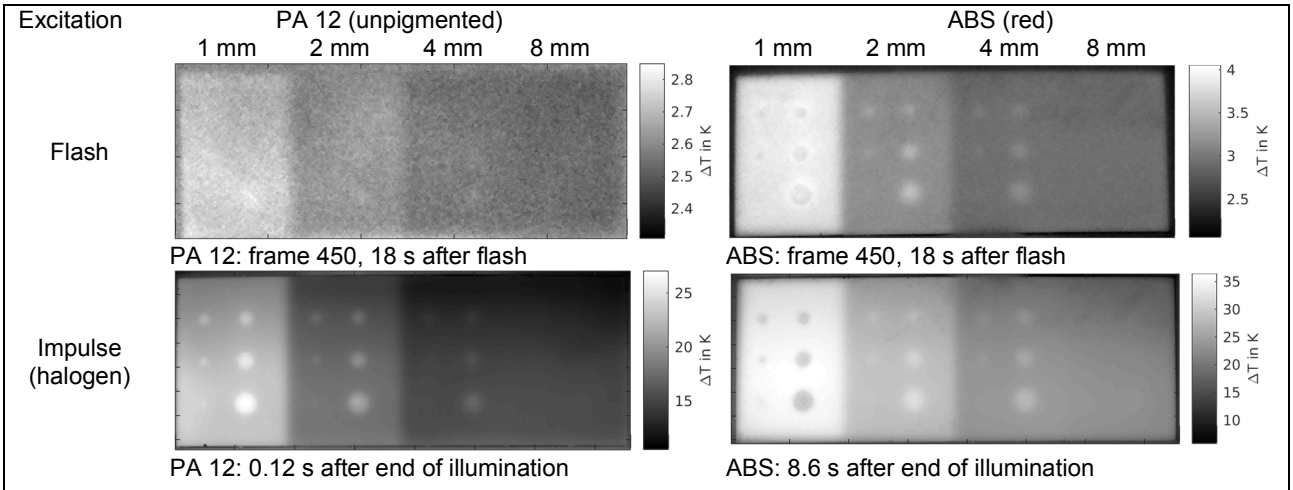

Fig. 4. *Thermograms of additively manufactured step wedges at the time of the maximum contrast of the deepest visible defects after excitation. Data processing: subtraction of zero images, appliance of hybrid-median-filtering.*

In all thermograms shown in figure 4, the mean of the first 7 images (instead of only one) was subtracted from all other images of that experiment (zero image correction). As next, for each thermogram a hybrid-median-filter (hmf) in space was applied [11]. This filter is a three-step ranking algorithm. It considers the nearest neighbouring pixels and one row after that. It firstly calculates the median of the four horizontal (H) and the four vertical (V) adjoining pixels. Secondly the median of the eight diagonal adjoining pixels (D) are calculated. At last, the median of the center pixel and the two calculated medians is the final value:

Table 2. *Scheme of categorizing pixels in a hmf.*

D	*	V	*	D
*	D	V	D	*
H	H	C	H	H
*	D	V	D	*
D	*	V	*	D

As the defects were centred in the steps in z-direction, the residual wall thickness increased with increasing step thickness: 0.2 mm, 0.7 mm, 1.7 mm and 3.7 mm for the 1 mm, 2 mm, 4 mm and 8 mm step, respectively, in the case of the 0.6 mm thick defects. In figure 4, it can be seen that PA 12 had a lower temperature increase after both, flash and impulse excitation with halogen lamps. One reason for this is the higher partial transparency compared to the red colored ABS (see figure 2). PA 12 is opaque for a smaller spectral range and therefore transformed less radiation energy into heat during excitation. At least the defects with a diameter of 8 mm, 6 mm, 5 mm and 4 mm in the 4 mm step (residual wall thickness: 1.7 mm) were detectable for both plastics and both ways of excitation, except for the PA 12 with flash excitation.

First derivative of the thermal signal reconstruction (TSR)

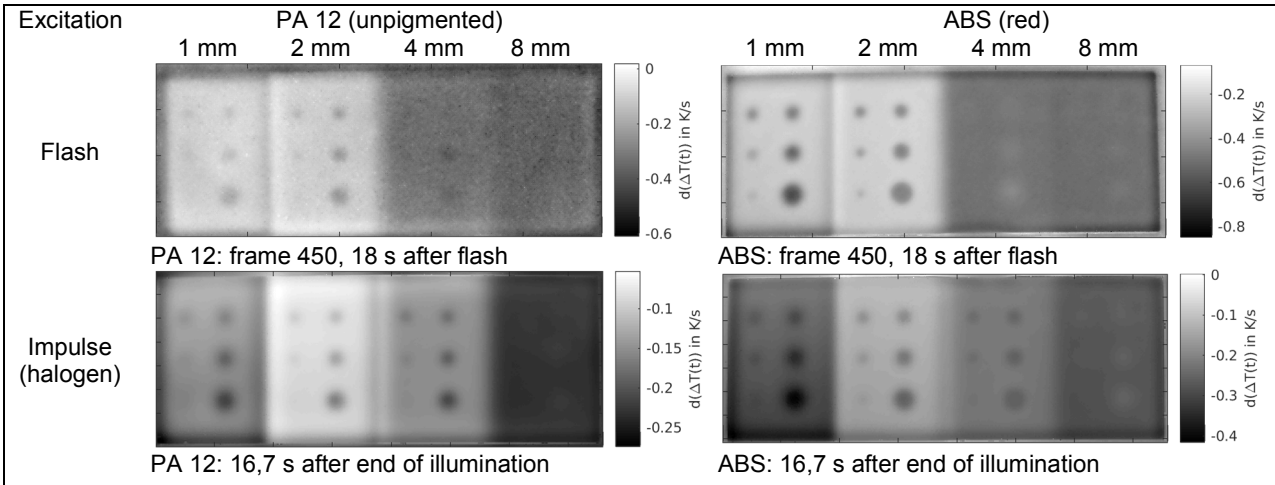

Fig. 5. *Images of the first, time derivative of the thermal sequences of additively manufactured step wedges at the time of the maximum contrast of the deepest visible defects after excitation. Data processing: subtraction of zero images, appliance of a hmf and calculation of the first derivative of the thermal signal reconstruction (TSR).*

If the whole recording time of the experiment is considered (240 s for flash and 160 s for impulse excitation), a thermal signal reconstruction (TSR) reduces noisy pixels and enhances the contrast [12]. Within a TSR the cooling curve of every pixel was transformed into double logarithmic scale and fitted with an eighth-degree polynomial. Subsequently, the first (figure 5) and second time derivatives (figure 6) were calculated. Selected images of the first derivative of the TSR show that the detectability of the defects was increased, see figure 5. For red colored ABS with halogen impulse excitation, the 8 mm diameter defect could be recognized, even in the 8 mm step with a residual wall thickness of 3.7 mm.

Second derivative of the thermal signal reconstruction (TSR)

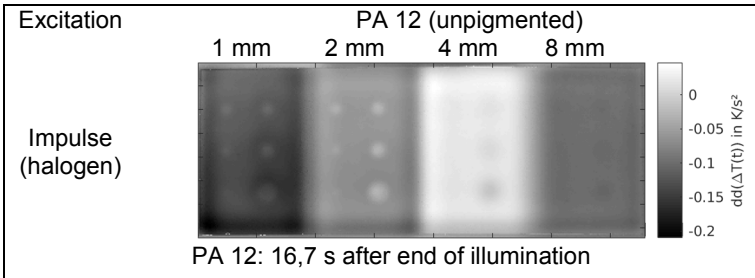

Fig. 6. *Thermogram the PA 12 step wedge at the time of the maximum contrast of the deepest visible defects after excitation. Data processing: subtraction of zero images, appliance of hmf and calculation of the second, time derivative of the TSR.*

The second derivative of the TSR also enables the detection of the defects with diameters of 8 mm, 6 mm, 5 mm in the 8 mm step in unpigmented PA 12 (figure 6).

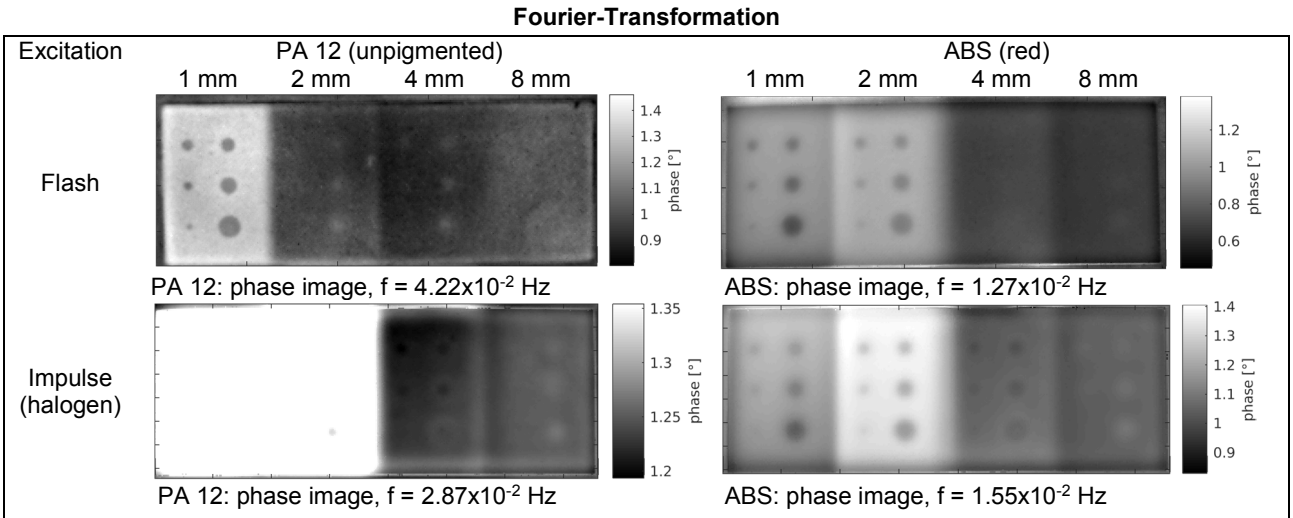

Fig. 7. *Phase images of the thermal sequences of additively manufactured step wedges. Data processing: subtraction of zero images, appliance of hmf, thermal signal reconstruction (TSR) and Fourier-Transformation. The frequency of the maximum contrast of the deepest visible defects after excitation is shown.*

As the TSR delivers the functions of the polynomials of the cooling curves, a Fourier-Transformation (FT) in time domain can be applied to these polynomials. This causes a transition from the time into the frequency domain, and phase images as well as amplitude images can be calculated (figure 7). In FT-images with low frequency, information from the whole time of the experiment can be found. After this data processing, the defects with a diameter of 8 mm, 6 mm, 5 mm in the 8 mm step could be detected for red colored ABS and unpigmented PA 12 with halogen impulse excitation (3.7 mm residual wall thickness).

5. Conclusion

These first results of the project clearly show, that active thermography can be used for the detection of defects in additively manufactured plastic parts.

It was found that a halogen impulse excitation with 30 seconds of illumination time suited better for PA 12 as well as for ABS than flash excitation (3 ms), to detect the imprinted artificial defects in the specimens. Furthermore, the detection of the defects in the 8 mm thick steps of the probes (remaining wall thickness of 3.7 mm) was possible by calculating the first derivative of the TSR as well as applying a Fourier-Transformation and considering the phase images at low frequencies for red pigmented ABS. Whereas, unpigmented PA 12 showed a better contrast in the defect regions in the second derivative of the TSR than in the first derivative. However, the phase images after a Fourier-Transformation allowed for the detection of the defects in the 8 mm thick step in the red colored ABS, the same way like they did for unpigmented PA 12.

Although the partially transparency is a great challenge for thermography, proper data processing like TSR, the calculation of derivatives as well as Fourier-Transformation enhances the quality of the results significantly. The results also indicate, that the partial transparency may decrease slightly in aged plastics, because the absorption properties change, which should be an advantage for the detection of defects with thermography in future experiments.

In general, colored plastics seem to be better for thermography, because the conversion of exciting radiation energy into heat is higher, than at unpigmented plastics.

The change of the properties with ongoing aging of plastics and possible synergic effects for testing methods, like for thermography, are still being investigated in the project.

Acknowledgements

This project is sponsored by the Federal Ministry for Economic Affairs and Energy due to a resolution of the German Parliament. IGF-Project 19151 N – "Non-destructive characterisation and quality assurance of the material properties and stability of additively manufactured plastics."

REFERENCES

[1] Wong K. V., Hernandez A., A Review of Additive Manufacturing. ISRN Mechanical Engineering; doi:10.5402/2012/208760, 2012.
[2] Guo N., Leu M. C., Additive manufacturing: technology, applications and research needs. Frontiers of Mechanical Engineering, - Vol. 8, No. 3, pp. 215 - 243, 2013.
[3] VDI-guidelinie VDI 3405, sheet 1, „Additive Fertigungsverfahren, Rapid Manufacturing - Laser-Sintern von Kunststoffbauteilen – Güteüberwachung". Beuth Verlag Berlin, Oktober 2013.
[4] Breuniger J., Becker R., Wolf A., Rommel S., Verl A., „Generative Fertigung mit Kunststoffen". Berlin, Heidelberg: Springer; 2013.
[5] Gebhardt A., „Additive Fertigungsverfahren", Hanser Verlag Munich, 5. edition, 711 pages, 2016.
[6] Turner B. N., Strong R., Gold S. A., "A review of melt extrusion additive manufacturing processes: I. Process design and modeling", Rapid Prototyping Journal, - Vol. 20, pp.192 - 204, 2014.
[7] DIN EN ISO 4892-3: 2014. „Kunststoffe – Künstliches Bestrahlen oder Bewittern in Geräten – Teil 3: UV-Leuchtstofflampen (ISO 4892-3:2013)"; German Edition EN ISO 4892-3:2013. Beuth Verlag.
[8] Chang S, "Analysis of Polymer Standards by Fourier Transform Infrared Spectroscopy-Attenuated Total Reflectance and Pyrolysis Gas Chromatography/Mass Spectroscopy and the Creation of Searchable Libraries". Research Report FSC 630 Forensic Science Internship Marshall University Forensic Science Program, 2012.
[9] Peydro M. A., Juarez D., Sanchez-Caballero S., Parres F., Study of the thermal properties acrylonitrile butadine styrene – high impact polystyrene blends with styrene ethylene butylene styrene. Annals of the Oradea University, Fascicle of Management and Technological Engineering, ISSUE #1, 2013.
[10] Altenburg S. J., Weber H., Krankenhagen R., Thickness determination of semitransparent solids using flash thermography and an analytical model. Quantitative InfraRed Thermography Journal. - Vol. 15, no 1, pp. 95 - 105, 2018.
[11] Hybrid-Median-Filter written by Damian Garcia 2007/2008 in MATLAB.
[12] Shepard S. M., Lhota J. R., Rubadeux B. A., Wang D., Ahmed T., Reconstruction and enhancement of active thermographic image sequences. Optical Engineering. - Vol. 42, No. 5, pp. 1337 - 1342, 2003.